



Published in final edited form as:

Nat Immunol. 2011 March ; 12(3): 213–221. doi:10.1038/ni.1992.

Germline *CYBB* mutations that selectively affect macrophages in kindreds with X-linked predisposition to tuberculous mycobacterial disease

Jacinta Bustamante^{1,2}, Andres A Arias^{3,17}, Guillaume Vogt^{4,17}, Capucine Picard^{1,2,5,6,17}, Lizbeth Blancas Galicia^{1,2,7}, Carolina Prando⁴, Audrey V Grant^{1,2}, Christophe C Marchal³, Marjorie Hubeau^{1,2}, Ariane Chappier^{1,2}, Ludovic de Beaucoudrey^{1,2}, Anne Puel^{1,2}, Jacqueline Feinberg^{1,2}, Ethan Valinetz³, Lucile Jannièrè^{1,2}, Céline Besse⁸, Anne Boland⁸, Jean-Marie Brisseau⁹, Stéphane Blanche⁶, Olivier Lortholary¹⁰, Claire Fieschi^{1,2,11}, Jean-François Emile¹², Stéphanie Boisson-Dupuis^{1,2,4}, Saleh Al-Muhsen¹³, Bruce Woda¹⁴, Peter E Newburger¹⁵, Antonio Condino-Neto¹⁶, Mary C Dinauer³, Laurent Abel^{1,2,4}, and Jean-Laurent Casanova^{1,2,4,6,13}

¹ Laboratory of Human Genetics of Infectious Diseases, Necker Branch, Institut National de la Santé et de la Recherche Médicale, U980, Paris, France

² Paris Descartes University, Necker Medical School, Paris, France

³ Wells Center for Pediatric Research, Department of Pediatrics, Indiana University School of Medicine, Indianapolis, Indiana, USA

⁴ St. Giles Laboratory of Human Genetics of Infectious Diseases, Rockefeller Branch, The Rockefeller University, New York, New York, USA

⁵ Center for the Study of Primary Immunodeficiencies, Assistance Publique–Hôpitaux de Paris AP-HP, Necker Hospital, Paris, France

⁶ Pediatric Hematology-Immunology Unit, Necker Hospital, Assistance Publique–Hôpitaux de Paris, Paris, France

⁷ National Institute of Pediatrics, Unit of Immunodeficiency, Mexico City, Mexico

⁸ National Genotyping Center, Evry, France

© 2011 Nature Americas, Inc. All rights reserved.

Correspondence should be addressed to J.-L.C. (jean-laurent.casanova@rockefeller.edu).

¹⁷These authors contributed equally to this work.

Note: Supplementary information is available on the Nature Immunology website.

AUTHOR CONTRIBUTIONS

J.B., L.A. and J.-L.C. designed the study and contributed intellectually to the experimental process; J.B. did most of the experiments under the supervision of J.-L.C.; A.A.A., C.C.M., E.V. and M.C.D. did the experiments with retroviral transduction of gp91^{phox} into EBV-B, CHO and PLB-985 cells; G.V. made the nonretroviral *CYBB* vectors, infected macrophages with BCG and made intellectual contributions to various experiments; C. Picard contributed to the recruitment of patients and initiated the clinical investigation; L.B.G., C. Prando, L.J. and M.H. analyzed many controls; A.C. did quantitative RT-PCR; L.d.B. did bioinformatics analysis; J.-F.E. did histological analysis of lymph nodes; B.W. did immunoperoxidase staining; A.V.G., C.B. and A.B. provided data for linkage analysis; A.P., J.F. and S.B.-D. provided experimental advice about cell culture; J.-M.B., S.B., O.L. and C.F. contributed to the recruitment and follow-up of the patients and CGD controls; S.A.-M., P.N., A.C.-N. and M.C.D. provided CGD controls and intellectual guidance for the development of various assays; J.B. and J.-L.C. wrote the paper; and all authors commented on and discussed the paper. B.W., P.E.N., A.C.-N. and M.C.D. contributed equally to this work.

COMPETING FINANCIAL INTERESTS

The authors declare no competing financial interests.

Published online at <http://www.nature.com/natureimmunology/>.

Reprints and permissions information is available online at <http://npg.nature.com/reprintsandpermissions/>.

⁹ Department of Internal Medicine, Nantes Hospital, Nantes, France

¹⁰ Department of Infectious Diseases, AP-HP, Necker Hospital, Paris, France

¹¹ Adult Immunopathology Unit, Saint Louis Hospital, Paris, France

¹² Department of Pathology, Institut National de la Santé et de la Recherche Médicale, U602, Ambroise Paré Hospital and Versailles Saint-Quentin-en-Yvelines University, Boulogne, France

¹³ Prince Naif Center for Immunology Research, Department of Pediatrics, College of Medicine, King Saud University, Riyadh, Saudi Arabia

¹⁴ Department of Pathology, University of Massachusetts Medical School, Worcester, Massachusetts, USA

¹⁵ Departments of Pediatrics and Cancer Biology, University of Massachusetts Medical School Worcester, Massachusetts, USA

¹⁶ Department of Immunology, Institute of Biomedical Sciences, University of São Paulo, São Paulo, Brazil

Abstract

Germline mutations in *CYBB*, the human gene encoding the gp91^{Phox} subunit of the phagocyte NADPH oxidase, impair the respiratory burst of all types of phagocytes and result in X-linked chronic granulomatous disease (CGD). We report here two kindreds in which otherwise healthy male adults developed X-linked recessive Mendelian susceptibility to mycobacterial disease (MSMD) syndromes. These patients had previously unknown mutations in *CYBB* that resulted in an impaired respiratory burst in monocyte-derived macrophages but not in monocytes or granulocytes. The macrophage-specific functional consequences of the germline mutation resulted from cell-specific impairment in the assembly of the NADPH oxidase. This ‘experiment of nature’ indicates that *CYBB* is associated with MSMD and demonstrates that the respiratory burst in human macrophages is a crucial mechanism for protective immunity to tuberculous mycobacteria.

Tuberculosis is a leading public health problem worldwide, and the study of genetic predisposition to tuberculosis is a promising avenue of research^{1,2}. Mendelian susceptibility to mycobacterial disease (MSMD; Mendelian Inheritance in Man accession code, 209950) is a rare syndrome that results in a predisposition to clinical disease caused by weakly virulent mycobacterial species, such as tuberculous *Mycobacterium bovis* bacillus Calmette-Guérin (BCG) vaccines and non-tuberculous, environmental mycobacteria^{1,3}. These patients are also vulnerable to more virulent *Mycobacterium tuberculosis*². Five disease-causing autosomal genes (*IFNGR1*, *IFNGR2*, *STAT1*, *IL12RB1* and *IL12B*) and one X-linked gene (*IKBK*G) have been identified³. Allelic heterogeneity accounts for the existence of 13 distinct disorders, all of which impair immunity mediated by interferon- γ (IFN- γ). The genetic etiology of about half of the patients with MSMD, however, remains unclear. Four maternally related French male patients (kindred A; patients P1–P4) presenting a second X-linked recessive form of MSMD (XR-MSMD-2) have been reported⁴. The patients had recurrent or disseminated tuberculous mycobacterial disease, with BCG disease in three patients (MSMD *sensu stricto*) and tuberculosis in one patient (not vaccinated by BCG). Another French kindred with XR-MSMD has been identified; the three male patients of this kindred (kindred B; patients P5–P7) had BCG disease. In patients from both kindreds, there was no distinguishable immunological phenotype, and the known etiologies of MSMD, including, in particular, X-linked mutations in *IKBK*G⁵, were excluded, which suggests that the two kindreds share a previously unknown X-linked recessive genetic etiology of MSMD.

RESULTS

***CYBB* mutations associated with MSMD**

Multipoint linkage analysis in the two kindreds described above (Supplementary Note) gave a maximum logarithm of odds score of 2.29 for two candidate regions on Xp11.3–Xp21.1 (13.83 megabases) and Xq25–Xq26.3 (11.79 megabases; Supplementary Fig. 1a). We excluded known X-linked primary immunodeficiencies on the basis of clinical and immunological grounds in both kindreds. We nonetheless sequenced the coding region of the primary immunodeficiency-causing genes present in those two chromosomal intervals in DNA isolated from the two probands (patients P4 in kindred A and P5 in kindred B). We found no mutations in *CD40LG* which encodes CD40L (CD154), the ligand for the costimulatory molecule CD40 (ref. 6), but we found, in exon 7 of *CYBB* in patient P4 from kindred A, a nucleotide substitution (A to C) in the codon encoding amino acid position 231 that resulted in the replacement of a glutamine by a proline residue (Q231P) in the gp91^{phox} subunit of the phagocyte NADPH oxidase, which is the protein encoded by *CYBB* (Fig. 1a,b). A nucleotide substitution (A to C) in the codon for amino acid position 178 that resulted in the replacement of a threonine by a proline residue (T178P) was present in exon 6 of *CYBB* in patient P5 from kindred B (Fig. 1a,b). Mutations in *CYBB* are commonly associated with chronic granulomatous disease (CGD)⁷, which defines the X-linked recessive form of CGD (XR-CGD). In both kindreds, the clinically affected male subjects were all hemizygous for the mutated allele, whereas the other maternally related, healthy male subjects tested were not. The eleven obligate female carriers tested in the two kindreds were heterozygous for the mutation, including a 90-year-old woman with a history of severe tuberculosis (H1), as well as four other female subjects (Fig. 1a). The strict familial cosegregation of *CYBB* genotype and MSMD phenotype (extended to tuberculosis) in the male subjects alive from both kindreds suggested that the *CYBB* mutations were responsible for disease. The mutations must have been transmitted by the male founders of both kindreds in generation, although they did not develop MSMD (Fig. 1a). However, these men lived in France before the introduction of routine BCG vaccination of children at a time when the incidence of tuberculosis was already decreasing.

The *CYBB* alleles encoding the Q231P and T178P substitutions were not present in any of 1,300 X chromosomes from 52 ethnic groups (in the panel from the Human Genome Diversity Project at the Centre d'Etude du Polymorphisme Humain), including 240 European chromosomes. Moreover, the two mutations were nonconservative, each resulting in substitution with a proline residue that is particularly disruptive (Fig. 1c) and affecting residues conserved in 33 animal species studied (Supplementary Fig. 1b). Finally, these two mutations have not previously been associated with CGD, a well-known primary immunodeficiency associated with many bacterial and fungal infectious diseases, including tuberculous mycobacterial diseases^{7–13} (Supplementary Note). All these observations are thus consistent with the proposal that the *CYBB* mutations resulting in Q231P and T178P are responsible for XR-MSMD-2 in these two kindreds.

Normal NADPH oxidase activity in circulating phagocytes

CYBB encodes the β -chain of flavocytochrome b₅₅₈ (also known as gp91^{phox} or NOX2), an essential element of the nicotinamide adenine dinucleotide phosphate (NADPH) oxidase complex (phox) in phagocytes such as granulocytes, monocytes and macrophages. It is also expressed, but to a lesser extent, in other cells, such as dendritic cells and B lymphocytes. In all phagocytes of patients with CGD or 'variant CGD', the production of reactive oxygen species is inadequate. To solve the paradox of *CYBB* mutations in two kindreds with MSMD but apparently not CGD or 'variant CGD' (Supplementary Note), we therefore investigated in depth the respiratory burst in the patients bearing the *CYBB* mutations resulting in Q231P

or T178P. Patient P4 had normal production of superoxide (O_2^-) and hydrogen peroxide (H_2O_2) in polymorphonuclear neutrophils (PMNs), as shown by the reduction of nitroblue tetrazolium (NBT) in response to endotoxin (lipopolysaccharide) and *Staphylococcus epidermidis*⁴ (data not shown). Moreover, the chemiluminescence of PMNs (a marker of both O_2^- and H_2O_2 concentration) stimulated with the phorbol ester PMA was also normal⁴. We obtained PMNs from the five patients tested and stimulated the cells with PMA in the presence or absence of catalase, then assessed their production of O_2^- by reduction of cytochrome *c* that can be inhibited by superoxide dismutase (a method for assessing specifically O_2^-). O_2^- production was in the normal range, even at early time points, and was proportional to the number of PMNs tested, even in the presence of catalase (Fig. 2a and Supplementary Fig. 2a,b). PMNs from the six patients tested also released H_2O_2 normally in response to PMA¹⁴ (Fig. 2b and Supplementary Fig. 2c). After PMA treatment, the O_2^- -dependent reduction of cytochrome *c* was normal in monocytes from the six patients tested (Fig. 2a and Supplementary Fig. 2d,e). Similar amounts of H_2O_2 were released after PMA activation of monocytes from the five patients tested and healthy controls, in contrast to the defect seen in monocytes from patients with CGD (Fig. 2b and Supplementary Fig. 2f). PMNs and monocytes from four heterozygous female subjects responded like control cells (Supplementary Fig. 2f).

In addition, we assessed functional respiratory burst activity by flow cytometry with dihydrorhodamine 123 to measure intracellular H_2O_2 production. PMNs and monocytes from patients P4 (kindred A) and P5 (kindred B) stimulated with PMA were normal (Fig. 2c and Supplementary Fig. 2g). Moreover, PMNs from patients P4 and P5 responded normally to milder activation involving priming with low concentrations of tumor necrosis factor, interleukin 1 β (IL-1 β) or cytochalasin b, followed by stimulation with the peptide formyl-Met-Leu-Phe (Fig. 2d and Supplementary Fig. 2h). Thus, the six patients bearing the mutated *CYBB* allele encoding the Q231P or T178P substitution had a normal respiratory burst in peripheral blood PMNs and monocytes, as assessed by diverse assays of O_2^- production and H_2O_2 release.

Finally, we searched for subtle functional defects that might have been missed by the experiments reported above by evaluating the *in vitro* killing of *Staphylococcus aureus* by granulocytes from one patient of each kindred. Their granulocytes killed *S. aureus* normally, unlike granulocytes from patients with CGD, in which *S. aureus* is the leading pathogen (Fig. 2e). These findings confirmed published investigations of these patients' respiratory burst⁴ and were consistent with the absence of clinical features typically associated with CGD and 'variant CGD', including staphylococcal disease, even in affected adults of advanced age from kindreds A and B⁴ (Fig. 1a).

Impaired NADPH oxidase activity in macrophages

In turn, the findings reported above raised the question of whether the two mutated *CYBB* alleles were pathogenic at all in the two kindreds with MSMD. We thus investigated the cellular basis of mycobacterial disease in these patients by assessing the oxidative function of their monocyte-derived macrophages (MDMs)^{15,16}. Tissue phagocytes, macrophages in particular, are the natural hosts of mycobacteria during the course of infection and disease. After 14–15 d of culture in the presence of macrophage colony-stimulating factor (M-CSF) to generate MDMs, H_2O_2 was detectable when control MDMs were cultured for 16–18 h with live BCG or PPD (purified protein derivative from *M. tuberculosis*) before PMA stimulation (Supplementary Fig. 3a). In the same conditions, macrophages from CGD patients P1, P2, P3 and P4 (Q231P; kindred A) released no detectable H_2O_2 . In similar conditions, but with interferon- γ (IFN- γ) rather than BCG or PPD, macrophages with the Q231P substitution also did not respond normally to the PMA trigger (Supplementary Fig. 3a). M-CSF-differentiated macrophages from patient P5 (T178P; kindred B) had a milder

phenotype, as they released low amounts or, in some conditions, normal amounts of H_2O_2 (Supplementary Fig. 3a). We also studied the deposition of formazan granules due to the reduction of NBT as a sensitive indicator of O_2^- production in individual macrophages derived from M-CSF-cultured monocytes. Only a very small fraction of BCG- or PPD-activated and PMA-triggered macrophages (less than 5%) from the four patients bearing the mutated allele encoding the Q231P substitution reduced NBT (Supplementary Fig. 3b). A larger fraction of macrophages from patient P5 bearing the mutated allele encoding the T178P substitution reduced NBT, but the results were strongly positive in less than 50%. As tissue macrophages from the patients were not available, we next tested MDMs derived *in vitro* in two conditions thought to reflect *in vivo* differentiation. We cultured MDMs with M-CSF alone for 7 d, then added lipopolysaccharide plus IFN- γ or IL-4. After 14–15 d of culture in either condition, MDMs from both patient P4 (kindred A) and patient P5 (kindred B) were unable to release detectable H_2O_2 , in contrast to control cells (Fig. 3 and Supplementary Fig. 3c). Thus, unlike blood granulocytes and monocytes, MDMs bearing the mutated *CYBB* allele encoding Q231P or T178P, in various conditions of *in vitro* differentiation and conditions of stimulation, showed impairment of the respiratory burst: the respiratory burst was almost abolished for cells with the Q231P substitution and severely impaired for those with the T178P substitution. We were unable to test the respiratory burst of the patients' macrophages *in vivo* or *ex vivo*.

We characterized the patients' macrophage defect further by assessing the growth of BCG in MDMs derived *in vitro* from two patients (P4 and P6) and ten healthy controls. As assessed by counting of colony-forming units, MDMs from the patients controlled BCG significantly less well than did control MDMs on day 14 ($P = 0.06$), and this difference was even greater on day 21 ($P = 0.003$; Supplementary Note and Supplementary Fig. 4). We observed no such difference in the presence of exogenous IFN- γ . These data provide a plausible mechanism for the cosegregation of the patients' *CYBB* mutation, the defect in their macrophage respiratory burst and their mycobacterial disease. As mycobacteria reside in macrophages *in vivo*, our *in vitro* experiments showing that MDMs in patients from each of the two kindreds had impairment of both the respiratory burst and the control of BCG growth provide a plausible cellular basis for the occurrence of mycobacterial diseases in patients with XR-MSMD-2.

Impaired NADPH activity in B cell lines

CYBB is expressed in some B cells. Although it is irrelevant to the pathogenesis of XR-MSMD-2, as B cell-deficient patients are not prone to mycobacterial diseases^{17,18}, we made use of this property to try to characterize the effects of the mutated *CYBB* alleles in Epstein Barr virus (EBV)-transformed B cell lines (EBV-B cells)¹⁹. After activation with PMA, EBV-B cells from 22 unrelated healthy people and nine male members of kindred A not carrying the *CYBB* mutation encoding Q231P were able to produce O_2^- (Fig. 4a and Supplementary Fig. 5). However, EBV-B cells from kindreds A and B (patients P1–P7), like cells from patients with XR-CGD, produced no detectable O_2^- (Fig. 4a and Supplementary Fig. 5). We then measured the release of H_2O_2 by EBV-B cells from patients P1–P7 after stimulation with various concentrations of PMA for various periods of time. None of the EBV-B cells from the seven patients released any detectable H_2O_2 , like those from XR-CGD patients (Fig. 4b). Only 1–3% of the cells from patients P1–P7 reduced NBT to formazan after activation with PMA (Fig. 4c). EBV-B cells and MDMs therefore shared a similar cellular phenotype. We transiently transfected EBV-B cells from a healthy control, a patient with XR-CGD, patient P4 (kindred A) and patient P5 (kindred B) with plasmid-encoded wild-type or mutated *CYBB* to determine whether the alleles encoding Q231P and T178P were functionally hypomorphic.

We next assessed functional reconstitution of the respiratory burst in assays of NBT reduction. At 48 h after transfection with wild-type *CYBB*, 10–13% of the cells from the patient with XR-CGD and patients P4 and P5 reduced NBT, but neither mock transfection nor transfection with either mutated *CYBB* allele had this effect (data not shown). We also established stable transfectants by means of a retroviral vector and quantified the respiratory burst by assessing H₂O₂ release. Stable transfection with the wild-type *CYBB* allele complemented the defect in EBV-B cells with the Q231P or T178P substitution (Fig. 4d), which indicated restoration of a functional respiratory burst in those cells and EBV-B cells from the patient with XR-CGD transduced with wild-type *CYBB*; however, we observed no complementation of the cellular phenotype (no detectable respiratory burst) in XR-CGD cells transduced with the allele encoding Q231P or T178P (Fig. 4d). Thus, EBV-B cells from these patients had an impaired respiratory burst because they carried the mutated *CYBB* allele encoding Q231P or T178P. The lack of a respiratory burst in peripheral B cells, by inference from results obtained with EBV-B cells, would not account for MSMD^{17,18}, but we demonstrated that a causal relationship between two mutants hemizygous for *CYBB* mutations encoding Q231P or T178P and impairment of the respiratory burst probably also applied to the patients' MDMs (treated with M-CSF plus IL4; Fig. 3), which could account for the clinical phenotype of MSMD. In contrast, these mutated *CYBB* alleles did not impair the respiratory burst of PMNs or monocytes (Fig. 2 and Supplementary Fig. 2), which explains the lack of the CGD or 'variant CGD' phenotype in the patients.

Impaired gp91^{phox} expression in macrophages

We also investigated the observed impairment in the functional respiratory burst in the patients' EBV-B cells and MDMs that was not present in PMNs or monocytes. We measured *CYBB* mRNA by real-time RT-PCR in four cell types from the five patients from the two kindreds tested and found it was similar to that in cells from five healthy controls (Supplementary Fig. 6a,b). We next investigated the cell-specific effect of the germline *CYBB* mutations encoding Q231P and T178P by assessing gp91^{phox} expression in the corresponding cells by immunoblot analysis with three specific antibodies (recognizing different epitopes on the gp91^{phox} protein) and increasing amounts of protein. PMNs produced the mutant Q231P gp91^{phox} protein in lower but detectable amounts (Fig. 5a and Supplementary Fig. 6c). Experiments with antibody 54.1 suggested that PMNs produced almost normal amounts of T178P gp91^{phox}, whereas experiments with the other two antibodies suggested that this protein was produced in smaller amounts, perhaps reflecting the nature of the epitopes recognized (Fig. 5a and Supplementary Fig. 6c). The abundance of the mutant Q231P gp91^{phox} protein was similarly low in monocytes, in which the abundance of the mutant T178P gp91^{phox} protein was also low but less affected (Fig. 5a,b). Notably, the defect in the expression of mutant Q231P or T178P gp91^{phox} protein was much greater in MDMs (Fig. 5b) and correlated with the greater defect in the respiratory burst in this cell type (Fig. 3 and Supplementary Fig. 3). However, we detected a species migrating at 65 kilodaltons (kDa) in the macrophage samples with the Q231P or T178P substitution (Fig. 5b). This size corresponded to the high-mannose gp65 precursor of gp91^{phox}, which may be more stable in macrophages than in monocytes or macrophages, as has been reported for EBV-B cells^{20,21}. This species is normally present only transiently in the endoplasmic reticulum before the incorporation of heme and formation of a heterodimer with p22^{phox} (another component of the NADPH oxidase complex), which is followed by additional carbohydrate processing of the *CYBB* subunit in the Golgi to the mature gp91^{phox} of about 91 kDa and ultimate targeting of flavocytochrome b₅₅₈ to post-biosynthetic membrane compartments^{22–26}. We also detected the gp65 species in a patient with XR-CGD (Fig. 5b) who has an L365P substitution in the flavin-binding domain but lacks gp91^{phox} expression and neutrophil oxidase activity²⁷. The presence of the gp65 intermediate suggests that these mutated alleles are associated with impaired formation of the heterodimer with

flavocytochrome b, which is required for the maturation of gp65 to gp91^{phox}. Finally, we did not have access to fresh tissue macrophages, but we did assess gp91^{phox} production by immunohistochemistry in the macrophages present in lymph node biopsy samples from two patients (Supplementary Fig. 6d,e). We found impaired gp91^{phox} production in macrophages from patient P4 (Q231P), as in lymph nodes from patients with CGD, but not in cells from healthy controls. We detected residual gp91^{phox} production in tissue PMNs from patient P4. As expected, we detected gp91^{phox} in both PMNs and macrophages from patient P5 (T178P). Together these data indicate that the patients' defect in gp91^{phox} expression was greater in macrophages than in neutrophils and monocytes and was overall more severe for the mutated *CYBB* allele encoding Q231P.

Impaired gp91^{phox} expression in EBV-B cells

We also tested EBV-B cells from a healthy control, a patient with XR-CGD (in this case, carrying complete deletion of the *CYBB* allele), and the patients with the Q231P and T178P mutant proteins, and those same cells transduced with wild-type *CYBB* or one of the mutated *CYBB* alleles (Fig. 5c). The two mutated *CYBB* alleles were poorly expressed in EBV-B cells, in which the 91-kDa form of gp91^{phox} was barely detectable in cells derived from patients or after transduction of XR-CGD cells with retroviral vector for expression of either mutated *CYBB* allele. Again, we detected a 65-kDa species corresponding to the high-mannose precursor of the mature 91-kDa form of gp91^{phox} for each of the Q231P and T178P mutants, in contrast to EBV-B cells from the patient with XR-CGD with a large deletion encompassing the entire *CYBB* gene (Fig. 5c).

We also investigated the expression of the other components of the NADPH oxidase complex. There was less p22^{phox} (which is encoded by *CYBA* and is normally bound to gp91^{phox}) in PMNs and EBV-B cells, particularly in cells with the Q231P substitution, paralleling gp91^{phox} expression (Supplementary Fig. 6f). Although expression of p22^{phox} in EBV-B cells is less affected by low or absent gp91^{phox} (ref. 28), p22^{phox} was still slightly lower in EBV-B cells from patients P4 and P5 (Supplementary Fig. 6g), which provided further, indirect evidence of impaired gp91^{phox} expression in the patients' EBV-B cells. The p47^{phox} and p67^{phox} subunits were expressed normally in patients' PMNs and EBV-B cells (Supplementary Fig. 6f,g). We observed reproducible differences between cell types in gp91^{phox} protein abundance for six patients carrying either Q231P or T178P, with less gp91^{phox} in MDMs and EBV-B cells than in the monocytes and PMNs, and different amounts in phagocytes and EBV-B cells from five controls, depending on the cell type. The *CYBB* mutation resulting in the Q231P substitution resulted in lower expression of gp91^{phox} protein *in vivo*, *ex vivo* and *in vitro* in granulocytes, monocytes, macrophages and EBV-B cells; steady-state amounts of this protein were determined in part by the cell type, with a greater effect in macrophages and EBV-B cells. There was higher expression of T178P gp91^{phox} protein, but it follows the same pattern according to the cell type. These expression data are consistent with the normal functional respiratory burst in the patients' PMNs and monocytes, in contrast to the functional defect in oxidant production by EBV-B cells and MDMs.

Impaired expression of flavocytochrome b₅₅₈

We then analyzed cell surface expression of the flavocytochrome b₅₅₈ complex (gp91^{phox} and p22^{phox}) on the plasma membrane by flow cytometry using monoclonal antibody (mAb) 7D5, which recognizes the motifs Ile-Lys-Asn-Pro (amino acids 160–163) and Arg-Ile-Val-Arg-Gly (amino acids 226–230) on gp91^{phox}, in the presence of p22^{phox} (refs. 29,30). Cell surface flavocytochrome b₅₅₈ was detectable in PMNs and monocytes from the two patients tested here, from two different kindreds, although less so for the Q231P mutant (Fig. 5d and Supplementary Fig. 6h). In contrast, flavocytochrome b₅₅₈ was almost undetectable on

EBV-B cells from seven patients tested among both kindreds (Fig. 5e). We obtained identical results for PMNs and EBV-B cells by spectrophotometry of absorption spectra (reduced – oxidized; Supplementary Fig. 6i). Adherent MDMs were not suitable for these two assays and we did not have access to fresh tissue macrophages. Analysis of the cell surface expression of flavocytochrome b_{558} in PMNs, monocytes and EBV-B cells from the heterozygous female subjects showed the presence of two discrete cell populations, those expressing and not expressing flavocytochrome b_{558} , correlating with both the functional respiratory burst and the inactivated X chromosome (Supplementary Fig. 7a,b and Supplementary Note). We obtained similar findings in NBT assays of MDMs from heterozygous female subjects (Supplementary Fig. 7c).

Thus, the Q231P and T178P substitutions impaired expression of the NADPH oxidase gp91^{phox} to a greater extent in MDMs and EBV-B cells than in PMNs and monocytes, showing a profound cell type-specific effect on the flavocytochrome b_{558} complex in terms of both surface and total expression. The relatively greater effect of the mutated alleles in MDMs and EBV-B cells may reflect cell type-related differences in the production of flavocytochrome b_{558} , which is greater in PMNs and monocytes than in MDMs or EBV-B cells^{19,31}. The much smaller amount of mutant gp91^{phox} protein in EBV-B cells and in MDMs, and possibly in tissue macrophages, severely limited the capacity for the assembly of a functional NADPH oxidase complex, whereas the amount produced by PMNs and monocytes, although smaller than normal, particularly for the Q213P allele, was sufficient to support the assembly of adequate amounts of the functional enzyme complex to produce normal amounts of oxidants^{32–35} (Fig. 2). Cell-type differences in the production of gp91^{phox} and the assembly of the flavocytochrome b_{558} heterodimer collectively account for the selective impairment of the respiratory burst in some cell types in the patients carrying the Q231P or T178P mutant protein.

Hypomorphic mutated *CYBB* alleles in Chinese hamster ovary cells

We additionally characterized the two mutated *CYBB* alleles encoding Q231P and T178P in a gp91^{phox}-deficient Chinese hamster ovary (CHO) epithelial cell line; this line lacks endogenous gp91^{phox}, which allows fine study of its biochemical processing and association with p22 (refs. 22–24,36–38). Unassembled subunits are more stable in CHO cells and other heterologous cells, as well as in EBV-B cells^{20,21,28}, than in granulocytes, where these are rapidly degraded by the cytosolic proteasome²³. The detection of the *CYBB*-encoded gp65 intermediate in macrophages and EBV-B cells from each kindred (Fig. 5b,c) suggested an underlying impairment in the maturation to gp91^{phox} that occurs after formation of the heterodimer with flavocytochrome *b*. We detected similar amounts of the gp65 form in CHO cells transduced with retroviral vector for the expression of wild-type or mutated *CYBB* alleles (encoding Q231P or T178P; Fig. 6a,b). The coexpression of wild-type p22^{phox} with wild-type *CYBB* resulted in a greater cellular abundance of mature 91-kDa gp91^{phox} (Fig. 6a,b). With coexpression of p22^{phox}, mature T178P gp91^{phox} was produced in almost normal amounts in the cell and on its surface, whereas Q231P gp91^{phox} was produced in much smaller quantities; for both mutated alleles, substantial gp65 precursor was still present (Fig. 6a,b). These findings suggest that there were no intrinsic problems in the stability of the gp65 precursors encoded by two *CYBB* missense alleles; instead, they provide further evidence that the products of these mutated alleles have less formation of the heterodimer with p22^{phox} and subsequent maturation to the mature gp91^{phox}, with the Q231P mutant being more severely hypomorphic than the T178P mutant, similar to the findings obtained with patients' myeloid cells.

Hypomorphic mutated *CYBB* alleles in PLB-985 cells

We then used an XR-CGD gp91^{phox}-deficient myelomonocytic PLB-985 cell line³⁵, which we also transduced with retroviral vector for constitutive expression of wild-type, Q231P or T178P gp91^{phox}. In the undifferentiated myelomonocytic cells, we detected gp91^{phox} in cells transduced with wild-type *CYBB*, whereas we detected only small amounts of gp91^{phox} after transduction with either of the mutated *CYBB* alleles, although the gp65 precursor was present (Fig. 6c). Mature T178P gp91^{phox} was again produced in larger amounts than Q231P gp91^{phox}. When we induced the cell line to differentiate into granulocytes, the two mutated alleles remained hypomorphic, with less gp91^{phox} (Fig. 6c). As found with fresh granulocytes from the patients, substantial respiratory burst activity relative to the amount of mature gp91^{phox} was supported by the mutated alleles in the granulocyte-differentiated cells (data not shown). In contrast, gp91^{phox} was not expressed by untransduced PLB-985 cells with a disrupted *CYBB* gene (PLB XR-CGD cells), in which no respiratory burst was detectable. We also examined endogenous and retrovirus-expressed gp91^{phox} after differentiation into monocyte-like or macrophage-like cells with either vitamin D³⁹ or a combination of vitamin D and PMA⁴⁰, respectively. In wild-type PLB-985 cells, there was more endogenous gp91^{phox} expression after treatment with either of these regimens (Fig. 6d). The expression of wild-type gp91^{phox} obtained through the use of constitutively active retroviral vector was similar in undifferentiated cells and after either type of differentiation (Fig. 6d). In contrast, retrovirus-mediated expression of T178P or Q231P gp91^{phox} was lower than that of wild-type gp91^{phox}, and it decreased even further after macrophage differentiation (Fig. 6d). These experiments demonstrated that the alleles encoding Q231P and T178P were hypomorphic in the myelomonocytic PLB-985 cell line. Although expression of the gp65 precursor of gp91^{phox} was preserved with either of the two mutations, there was lower but not abolished expression of gp91^{phox} itself, consistent with impaired formation of flavocytochrome b₅₅₈, particularly after macrophage differentiation.

DISCUSSION

We have reported here germline mutations in *CYBB* conferring the phenotype of XR-MSMD but not XR-CGD or ‘variant XR-CGD’. Six otherwise healthy and maternally related male adults with BCG disease and another with true tuberculosis had XR-MSMD-2 due to inheritance of a mutated *CYBB* allele encoding a Q231P or T178P substitution. The two missense mutations were intrinsically and severely hypomorphic in gp91^{phox}-deficient cells as diverse as EBV-B cells, CHO cells and PLB-985 cells. *CYBB* is a Mendelian gene encoding susceptibility to mycobacteria, the seventh gene identified causing MSMD and second gene identified causing XR-MSMD, and the fifth gene resulting in a predisposition to tuberculosis (after *IFNGR1*, *IL12B*, *IL12RB1* and *IKBKKG*)^{2,3}. We have shown here that it affects the respiratory burst. The physiological links between *CYBB* and the formerly identified MSMD-causing and tuberculosis-predisposing genes involved in the IL-12–IFN- γ circuit remain to be elucidated. The cellular phenotype of this defect is uniform and different from that of CGD and ‘variant CGD’: the respiratory burst in MDMs or EBV-B cells from the seven patients tested was severely impaired, whereas their PMNs and monocytes showed no such dysfunction. The *CYBB* alleles encoding Q231P and T178P are therefore hypomorphic in a cell-specific manner and provide an example of a human genetic illness resembling the phenotype of mice with conditional knockout of *Cybb*, with the nuance that gene ablation in one of the two affected lineages also depends on cell differentiation (monocyte to macrophage). *CYBB* is a human gene for which alleles that are null in all cells (in particular all phagocytes, resulting in XR-CGD) and now in selected cell types (in particular in macrophages, resulting in MSMD) have been identified and shown to produce different phenotypes. The mechanism underlying the B cell- and macrophage-specific effects of these germline mutations, which resulted in impaired but not absent assembly of

flavocytochrome b₅₅₈, is related to cell-specific differences in gp91^{phox} expression, in the threshold of gp91^{phox} expression required for assembly of the flavocytochrome b₅₅₈ complex, and in the threshold of assembled b₅₅₈ complex required for NADPH oxidase activity. The clear-cut dichotomy between cells with an entirely normal respiratory burst (PMNs and monocytes) and those with a severely impaired respiratory burst (MDMs and EBV-B cells) was notable. Further studies are needed to test the effect of these two mutations on the respiratory burst of dendritic cells⁴¹.

Our study suggests that the respiratory burst in human tissue macrophages is critical for immunity to tuberculous mycobacteria. It is already apparent from human patients with CGD¹¹ that the respiratory burst has an important role in immunity to BCG and *M. tuberculosis*. Notably, such patients are not prone to infection with environmental, non-tuberculous mycobacteria, even with species more virulent than BCG in other patients with MSMD, which indicates that the respiratory burst is redundant for the macrophage destruction of most non-tuberculous mycobacteria. The growth of BCG was enhanced in the patients' MDMs *in vitro*, which further suggests that there is a specific requirement for assembly of the NADPH oxidase in the control of tuberculous mycobacteria in human macrophages *in vivo*. Other pathways possibly disrupted by impairment of the respiratory burst in macrophages, such as IL-12 production, may also contribute to the pathogenesis of mycobacterial diseases. The role of the respiratory burst in antimycobacterial immunity *in vivo* and *in vitro* has not been firmly established in the mouse model, in which nitric oxide has a much more important role^{42–45}. Further genetic approaches^{46,47} may demonstrate the means by which the human respiratory burst controls tuberculous mycobacteria and the role of nitric oxide production in combating tuberculous or non-tuberculous mycobacteria⁴⁵. Conversely, our seven adult patients with MSMD (including a patient with tuberculosis) were clinically healthy and had no history of other granulomatous or infectious diseases. This suggests that both the granulomatous disease and the bacterial and fungal infections affecting patients with CGD or 'variant CGD' reflect additional dysfunctions of granulocytes and/or monocytes rather than macrophage defects alone^{48,49}.

METHODS

Methods and any associated references are available in the online version of the paper at <http://www.nature.com/natureimmunology/>.

Supplementary Material

Refer to Web version on PubMed Central for supplementary material.

Acknowledgments

We thank the family members for participating in this study; J. Curnutte (3-V Biosciences) for EBV-B cells from CGD controls; D. Roos (University of Amsterdam) for mAb 449; F. Morel (Grenoble University) for mAb 7A2; M. Quinn (Montana State University) for mAb 54.1; all members of the two branches of the laboratory of Human Genetics of Infectious Diseases for discussions; and T. Leclerc, Y. Rose, M. de Suremain, M. Kezadi, and N. Stull for technical assistance. Supported by Institut National de la Santé et de la Recherche Médicale (J.B.), the European Union (NEOTIM EEA05095KKA to J.B., and HOMITB HEALTH-F3-2008-200732), the March of Dimes (RO5050KK to J.B.), Fundação de Amparo a Pesquisa do Estado de São Paulo (A.C.-N.), Conselho Nacional de Desenvolvimento Científico e Tecnológico (A.C.-N.), Fondation BNP-Paribas, Fondation Schlumberger, Institut Universitaire de France, Agence Nationale de Recherche, The Rockefeller University Center for Clinical and Translational Science (SUL1RR024143-03), The Rockefeller University, the National Institutes of Health (AI 079788 and DK54369 to P.E.N., and HL045635 to M.C.D.), the Riley Children's Foundation (M.C.D.) and the Howard Hughes Medical Institute (J.-L.C.).

References

1. Casanova JL, Abel L. Genetic dissection of immunity to mycobacteria: the human model. *Annu Rev Immunol.* 2002; 20:581–620. [PubMed: 11861613]
2. Alcais A, Fieschi C, Abel L, Casanova JL. Tuberculosis in children and adults: two distinct genetic diseases. *J Exp Med.* 2005; 202:1617–1621. [PubMed: 16365144]
3. Filipe-Santos O, et al. Inborn errors of IL-12/23- and IFN- γ -mediated immunity: molecular, cellular, and clinical features. *Semin Immunol.* 2006; 18:347–361. [PubMed: 16997570]
4. Bustamante J, et al. A novel X-linked recessive form of Mendelian susceptibility to mycobacterial disease. *J Med Genet.* 2007; 44:e65. [PubMed: 17293536]
5. Filipe-Santos O, et al. X-linked susceptibility to mycobacteria is caused by mutations in NEMO impairing CD40-dependent IL-12 production. *J Exp Med.* 2006; 203:1745–1759. [PubMed: 16818673]
6. Notarangelo LD, et al. Primary immunodeficiencies: 2009 update. *J Allergy Clin Immunol.* 2009; 124:1161–1178. [PubMed: 20004777]
7. Roos D, et al. Hematologically important mutations: X-linked chronic granulomatous disease (third update). *Blood Cells Mol Dis.* 2010; 45:246–265. [PubMed: 20729109]
8. Mouy R, Fischer A, Vilmer E, Seger R, Griscelli C. Incidence, severity, and prevention of infections in chronic granulomatous disease. *J Pediatr.* 1989; 114:555–560. [PubMed: 2784499]
9. Segal BH, Leto TL, Gallin JI, Malech HL, Holland SM. Genetic, biochemical, and clinical features of chronic granulomatous disease. *Medicine (Baltimore).* 2000; 79:170–200. [PubMed: 10844936]
10. Winkelstein JA, et al. Chronic granulomatous disease. Report on a national registry of 368 patients. *Medicine (Baltimore).* 2000; 79:155–169. [PubMed: 10844935]
11. Bustamante J, et al. BCG-osis and tuberculosis in a child with chronic granulomatous disease. *J Allergy Clin Immunol.* 2007; 120:32–38. [PubMed: 17544093]
12. Lee PP, et al. Susceptibility to mycobacterial infections in children with X-linked chronic granulomatous disease: a review of 17 patients living in a region endemic for tuberculosis. *Pediatr Infect Dis J.* 2008; 27:224–230. [PubMed: 18277931]
13. van den Berg JM, et al. Chronic granulomatous disease: the European experience. *PLoS ONE.* 2009; 4:e5234. [PubMed: 19381301]
14. Mohanty JG, Jaffe JS, Schulman ES, Raible DG. A highly sensitive fluorescent micro-assay of H₂O₂ release from activated human leukocytes using a dihydroxyphenoxazine derivative. *J Immunol Methods.* 1997; 202:133–141. [PubMed: 9107302]
15. Nakagawara A, Nathan CF, Cohn ZA. Hydrogen peroxide metabolism in human monocytes during differentiation in vitro. *J Clin Invest.* 1981; 68:1243–1252. [PubMed: 6271809]
16. Martinez FO, Gordon S, Locati M, Mantovani A. Transcriptional profiling of the human monocyte-to-macrophage differentiation and polarization: new molecules and patterns of gene expression. *J Immunol.* 2006; 177:7303–7311. [PubMed: 17082649]
17. Reichenbach J, et al. Mycobacterial diseases in primary immunodeficiencies. *Curr Opin Allergy Clin Immunol.* 2001; 1:503–511. [PubMed: 11964733]
18. Conley ME, et al. Primary B cell immunodeficiencies: comparisons and contrasts. *Annu Rev Immunol.* 2009; 27:199–227. [PubMed: 19302039]
19. Condino-Neto A, Newburger PE. NADPH oxidase activity and cytochrome b558 content of human Epstein-Barr-virus-transformed B lymphocytes correlate with expression of genes encoding components of the oxidase system. *Arch Biochem Biophys.* 1998; 360:158–164. [PubMed: 9851826]
20. Porter CD, et al. p22-phox-deficient chronic granulomatous disease: reconstitution by retrovirus-mediated expression and identification of a biosynthetic intermediate of gp91-phox. *Blood.* 1994; 84:2767–2775. [PubMed: 7919388]
21. Maly FE, et al. Restitution of superoxide generation in autosomal cytochrome-negative chronic granulomatous disease (A22(0) CGD)-derived B lymphocyte cell lines by transfection with p22phox cDNA. *J Exp Med.* 1993; 178:2047–2053. [PubMed: 8245781]
22. Yu L, et al. Biosynthesis of flavocytochrome b558. gp91^{phox} is synthesized as a 65-kDa precursor (p65) in the endoplasmic reticulum. *J Biol Chem.* 1999; 274:4364–4369. [PubMed: 9933639]

23. DeLeo FR, et al. Processing and maturation of flavocytochrome b558 include incorporation of heme as a prerequisite for heterodimer assembly. *J Biol Chem.* 2000; 275:13986–13993. [PubMed: 10788525]
24. Yu L, Zhen L, Dinauer MC. Biosynthesis of the phagocyte NADPH oxidase cytochrome b558. Role of heme incorporation and heterodimer formation in maturation and stability of gp91phox and p22phox subunits. *J Biol Chem.* 1997; 272:27288–27294. [PubMed: 9341176]
25. Nakamura M, Murakami M, Koga T, Tanaka Y, Minakami S. Monoclonal antibody 7D5 raised to cytochrome b558 of human neutrophils: immunocytochemical detection of the antigen in peripheral phagocytes of normal subjects, patients with chronic granulomatous disease, and their carrier mothers. *Blood.* 1987; 69:1404–1408. [PubMed: 3552074]
26. Biberstine-Kinkade KJ, et al. Heme-ligating histidines in flavocytochrome b(558): identification of specific histidines in gp91^{phox}. *J Biol Chem.* 2001; 276:31105–31112. [PubMed: 11413138]
27. Heyworth PG, et al. Hematologically important mutations: X-linked chronic granulomatous disease (second update). *Blood Cells Mol Dis.* 2001; 27:16–26. [PubMed: 11162142]
28. Porter CD, Kuribayashi F, Parkar MH, Roos D, Kinnon C. Detection of gp91-phox precursor protein in B-cell lines from patients with X-linked chronic granulomatous disease as an indicator for mutations impairing cytochrome b558 biosynthesis. *Biochem J.* 1996; 315:571–575. [PubMed: 8615831]
29. Yamauchi A, et al. Location of the epitope for 7D5, a monoclonal antibody raised against human flavocytochrome b558, to the extracellular peptide portion of primate gp91phox. *Microbiol Immunol.* 2001; 45:249–257. [PubMed: 11345535]
30. Burritt JB, et al. Phage display epitope mapping of human neutrophil flavocytochrome b558. Identification of two juxtaposed extracellular domains. *J Biol Chem.* 2001; 276:2053–2061. [PubMed: 11027685]
31. Cassatella MA, et al. Molecular basis of interferon- γ and lipopolysaccharide enhancement of phagocyte respiratory burst capability. Studies on the gene expression of several NADPH oxidase components. *J Biol Chem.* 1990; 265:20241–20246. [PubMed: 2173701]
32. Ezekowitz RA, Dinauer MC, Jaffe HS, Orkin SH, Newburger PE. Partial correction of the phagocyte defect in patients with X-linked chronic granulomatous disease by subcutaneous interferon γ . *N Engl J Med.* 1988; 319:146–151. [PubMed: 2838754]
33. Ding C, et al. High-level reconstitution of respiratory burst activity in a human X-linked chronic granulomatous disease (X-CGD) cell line and correction of murine X-CGD bone marrow cells by retroviral-mediated gene transfer of human gp91phox. *Blood.* 1996; 88:1834–1840. [PubMed: 8781441]
34. Ezekowitz RA, et al. Restoration of phagocyte function by interferon- γ in X-linked chronic granulomatous disease occurs at the level of a progenitor cell. *Blood.* 1990; 76:2443–2448. [PubMed: 2176110]
35. Zhen L, et al. Gene targeting of X chromosome-linked chronic granulomatous disease locus in a human myeloid leukemia cell line and rescue by expression of recombinant gp91phox. *Proc Natl Acad Sci USA.* 1993; 90:9832–9836. [PubMed: 8234321]
36. Casbon AJ, Allen LA, Dunn KW, Dinauer MC. Macrophage NADPH oxidase flavocytochrome B localizes to the plasma membrane and Rab11-positive recycling endosomes. *J Immunol.* 2009; 182:2325–2339. [PubMed: 19201887]
37. Zhu Y, et al. Deletion mutagenesis of p22phox subunit of flavocytochrome b558: identification of regions critical for gp91phox maturation and NADPH oxidase activity. *J Biol Chem.* 2006; 281:30336–30346. [PubMed: 16895900]
38. Biberstine-Kinkade KJ, et al. Mutagenesis of p22^{phox} histidine 94. A histidine in this position is not required for flavocytochrome b558 function. *J Biol Chem.* 2002; 277:30368–30374. [PubMed: 12042318]
39. Perkins SL, Link DC, Kling S, Ley TJ, Teitelbaum SL. 1,25-Dihydroxyvitamin D3 induces monocytic differentiation of the PLB-985 leukemic line and promotes c-fgr mRNA expression. *J Leukoc Biol.* 1991; 50:427–433. [PubMed: 1660912]

40. Jitkaew S, Witasp E, Zhang S, Kagan VE, Fadeel B. Induction of caspase- and reactive oxygen species-independent phosphatidylserine externalization in primary human neutrophils: role in macrophage recognition and engulfment. *J Leukoc Biol.* 2009; 85:427–437. [PubMed: 19106181]
41. Savina A, et al. NOX2 controls phagosomal pH to regulate antigen processing during crosspresentation by dendritic cells. *Cell.* 2006; 126:205–218. [PubMed: 16839887]
42. Adams LB, Dinauer MC, Morgenstern DE, Krahenbuhl JL. Comparison of the roles of reactive oxygen and nitrogen intermediates in the host response to *Mycobacterium tuberculosis* using transgenic mice. *Tuber Lung Dis.* 1997; 78:237–246. [PubMed: 10209678]
43. Segal BH, et al. The p47(phox^{-/-}) mouse model of chronic granulomatous disease has normal granuloma formation and cytokine responses to *Mycobacterium avium* and *Schistosoma mansoni* eggs. *Infect Immun.* 1999; 67:1659–1665. [PubMed: 10085000]
44. Nathan C, Shiloh MU. Reactive oxygen and nitrogen intermediates in the relationship between mammalian hosts and microbial pathogens. *Proc Natl Acad Sci USA.* 2000; 97:8841–8848. [PubMed: 10922044]
45. MacMicking J, Xie QW, Nathan C. Nitric oxide and macrophage function. *Annu Rev Immunol.* 1997; 15:323–350. [PubMed: 9143691]
46. Casanova JL, Abel L. Primary immunodeficiencies: a field in its infancy. *Science.* 2007; 317:617–619. [PubMed: 17673650]
47. Alcais A, Abel L, Casanova JL. Human genetics of infectious diseases: between proof of principle and paradigm. *J Clin Invest.* 2009; 119:2506–2514. [PubMed: 19729848]
48. Gordon S, Taylor PR. Monocyte and macrophage heterogeneity. *Nat Rev Immunol.* 2005; 5:953–964. [PubMed: 16322748]
49. Segal AW. How neutrophils kill microbes. *Annu Rev Immunol.* 2005; 23:197–223. [PubMed: 15771570]

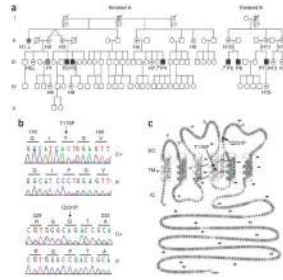


Figure 1.

CYBB mutations encoding Q231P and T178P substitutions in XR-MSMD-2. **(a)** Pedigrees of the families with XR-MSMD-2, including only those selected for the X-chromosome scan. I–V (left margin) indicate generations; black symbols indicate patients with BCG disease (P2–P7); gray symbols indicate patients with tuberculosis (P1 and H1); arrows indicate probands; black dots indicate heterozygous female subjects ($n = 15$); vertical bars indicate the two founders who must have carried the *CYBB* mutation but did not show any mycobacterial phenotype; ‘E?’ indicates those whose genetic status could not be evaluated; white indicates all other family members (wild-type *CYBB*). **(b)** Automated sequencing profile showing the *CYBB* mutations encoding the Q231P and T178P substitutions in cDNA extracted from EBV-B cells from patients (P) and a control (C+). The mutations were confirmed in genomic DNA and cDNA for seven patients. **(c)** Topology model of gp91^{phox} regions corresponding to the extracellular (EC), transmembrane (TM) and intracellular (IC) regions. Q231P is in the third extracellular loop and T178P is in the transmembrane region (red dots).

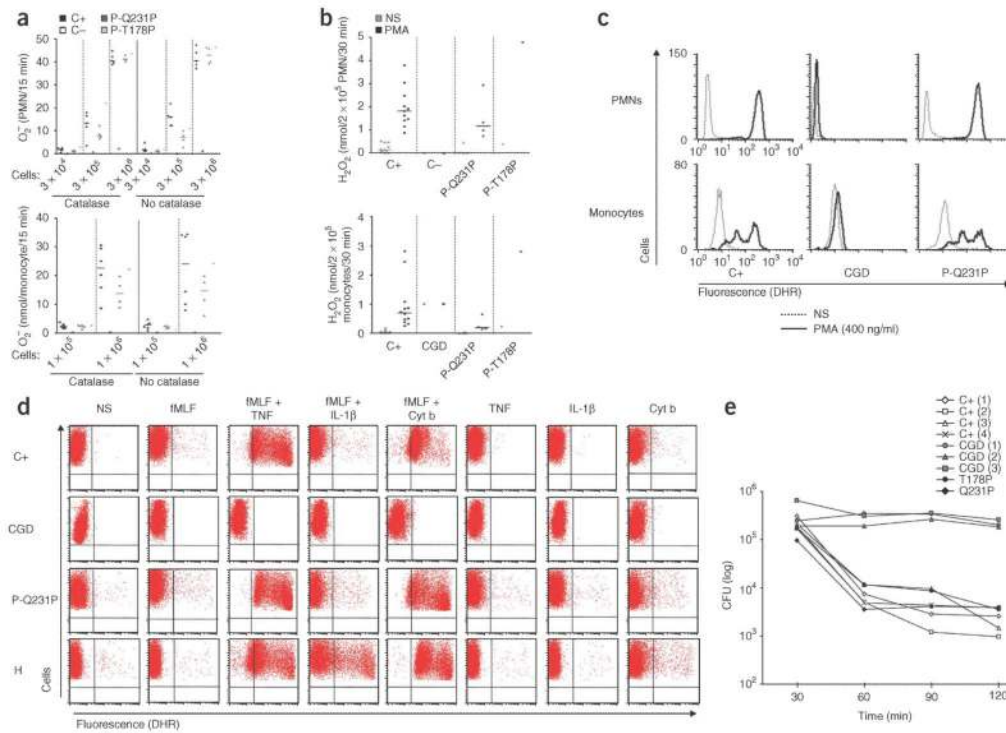


Figure 2.

NADPH oxidase activity in PMNs and monocytes. **(a)** O_2^- generation in PMNs and monocytes from healthy controls (C+; $n = 5$ (PMNs) and $n = 6$ (monocytes)), a patient with CGD (CGD; $n = 1$) and patients with the *CYBB* mutations (P-Q231P ($n = 4$) and P-T178P ($n = 1$)), assessed after the addition of PMA (40 ng/ml) with or without catalase (ten conditions: six for PMNs and four for monocytes), measured by an assay for reduction of cytochrome *c* that can be inhibited by superoxide dismutase. Each symbol represents an individual subject. $P = 0.01$ (not significant), healthy controls versus patients with the Q231P substitution (nonparametric Wilcoxon exact test, accounting for multiple testing). **(b)** Fluorometric quantification of H_2O_2 release from PMNs and monocytes from healthy controls ($n = 11$ (PMNs) and $n = 12$ (monocytes)) and in patients with CGD or the *CYBB* mutations, assessed with the fluorogenic substrate ADHP (*N*-acetyl-3,7-dihydroxyphenoxazine) after the addition of PMA. **(c)** Flow cytometry of intracellular H_2O_2 production (dihydrorhodamine 123 (DHR) assay) in PMNs and monocytes from healthy controls, a patient with X-linked CGD and a patient with the Q231P substitution, assessed before (dotted lines) and after (solid lines) stimulation with PMA (400 ng/ml). **(d)** Flow cytometry (dihydrorhodamine 123 assay) of PMNs from healthy controls, patients with CGD, a patient with the Q231P substitution and a female heterozygous for the allele encoding Q231P (H), left untreated (NS) or treated with various combinations (above plots) of tumor necrosis factor (TNF), IL-1 β , cytochalasin b (Cyt b) and formyl-Met-Leu-Phe (fMLF). **(e)** Killing of *S. aureus* by granulocytes from healthy controls ($n = 4$; 1–4 in parentheses), patients with CGD ($n = 3$; 1–3 in parentheses) and a patient from kindred A (Q231P; $n = 1$) and one from kindred B (T178P; $n = 1$). CFU, colony-forming units. Data are representative of three experiments (**a,b**; mean of duplicates in **b**), two experiments (**c,e**) or two independent experiments (**d**).

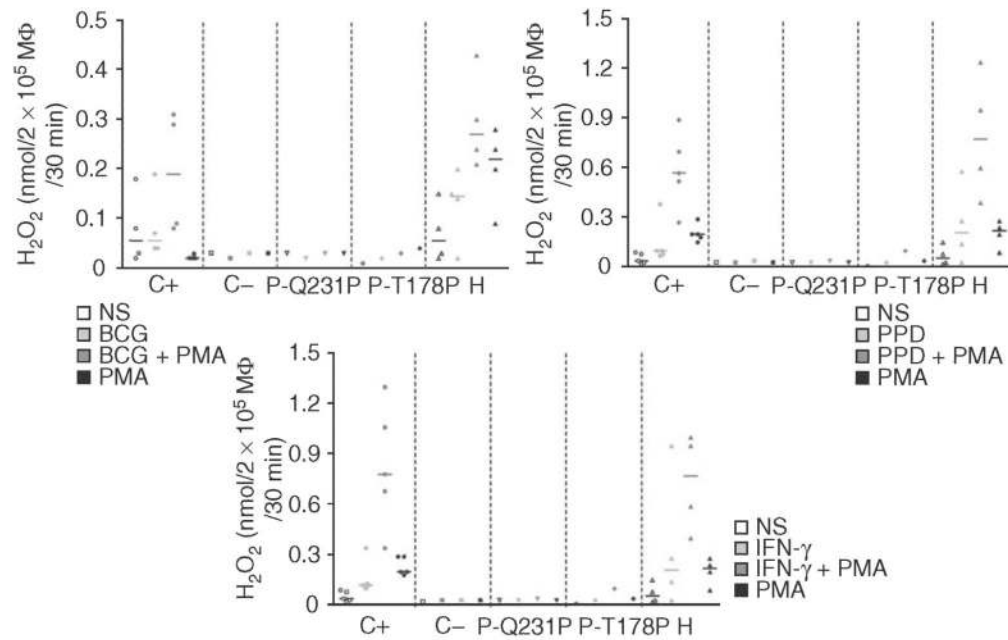


Figure 3. NADPH oxidase activity in MDMs. Release of H₂O₂ from MDMs (MΦ) obtained from healthy controls ($n = 4$), a patient with X-linked CGD ($n = 1$), patients with the *CYBB* mutations (Q231P ($n = 1$) and T178P ($n = 1$)), and females heterozygous for the *CYBB* mutations ($n = 4$), then left untreated (NS) or treated with M-CSF and IL-4 and then activated by incubation for 18 h with live BCG (10:1 (BCG:MDM); left), PPD (1 mg/ml; right) or IFN- γ (1×10^5 IU/ml; bottom), followed by no trigger or by treatment with PMA (400 ng/ml) to trigger H₂O₂ release (+PMA). Each symbol represents an individual subject. Data are representative of two independent experiments.

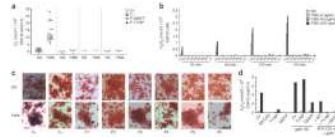
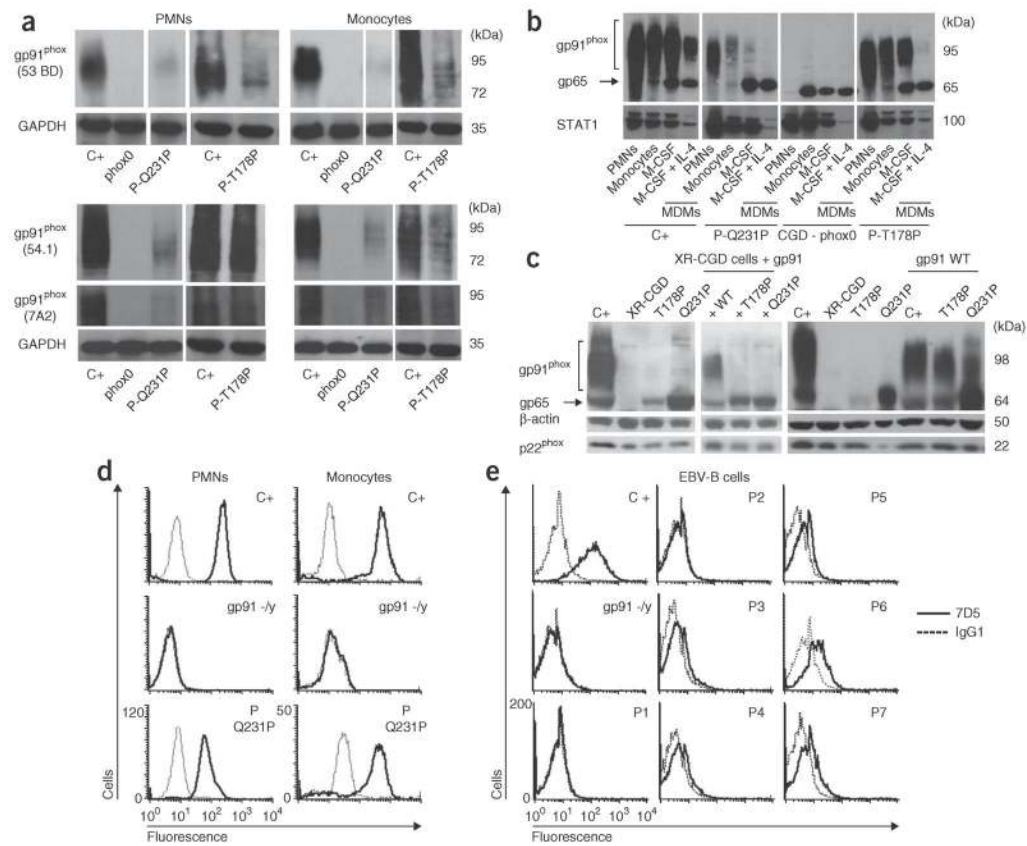
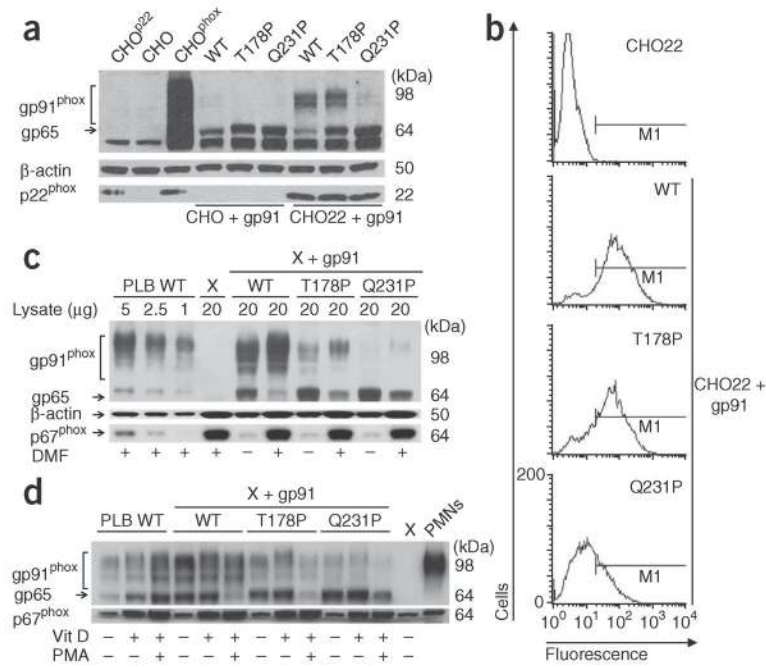


Figure 4.

NADPH oxidase activity in EBV-B cells. **(a)** O_2^- production (cytochrome *c* reduction) by EBV-B cells (1×10^6) obtained from healthy controls ($n = 22$), patients with XR-CGD ($n = 4$) and patients with the *CYBB* mutations (Q231P ($n = 4$) and T178P ($n = 3$)), then activated by incubation for 2 h with PMA (400 ng/ml). Each symbol represents an individual subject. **(b)** H_2O_2 release by EBV-B cells obtained from a healthy control, patients P1–P7 and a patient with XR-CGD, activated with various doses of PMA (key) at four time points (horizontal axis). **(c)** NBT reduction by EBV-B cells from a healthy control, patients P1–P6 and a patient with X-linked CGD, assessed before (NS) and after (PMA) activation with PMA (400 ng/ml). Original magnification, $\times 100$. **(d)** NADPH oxidase function in EBV-B cells from a patient with XR-CGD transduced with retroviral particles encoding wild-type gp91^{phox} (WT), T178P gp91^{phox} and Q231P gp91^{phox}, and EBV-B cells obtained from patients with the T178P substitution and a healthy control transduced with retroviral particles encoding wild-type gp91^{phox}, assessed as H_2O_2 release after 2 h of PMA activation (400 ng/ml). Data are representative of two independent experiments (**a,d**) or three experiments (**b,c**).

**Figure 5.**

Expression of gp91^{phox} and flavocytochrome b₅₅₈. **(a)** Immunoblot analysis of PMNs and monocytes from a healthy control, a patient with no gp91^{phox} protein (phox0) and patients with the *CYBB* mutations, probed with three antibodies to gp91^{phox} (53 BD, 54.1 and 7A2) and an antibody to GAPDH (glyceraldehyde phosphate dehydrogenase; loading control). Right margin, molecular size in kDa. **(b)** Immunoblot analysis of PMNs, monocytes and MDMs (treated with M-CSF alone or M-CSF plus IL-4) from a healthy control, a patient with CGD and no gp91^{phox0} (CGD-phox0) and patients with the *CYBB* mutations, probed with mAb 54.1 to gp91^{phox} and an antibody to the transcription factor STAT1 (loading control). **(c)** Immunoblot analysis of lysates of EBV-B cells from a healthy control, a patient with XR-CGD and patients with the *CYBB* mutations (left), EBV-B cells from the same patient with XR-CGD transduced with wild-type gp91^{phox}, T178P gp91^{phox} or Q231P gp91^{phox} retroviral particles (middle), or EBV-B cells as described for the far left blot, left untransduced (left) or transduced (right; except XR-CGD) with wild-type gp91^{phox} retroviral particles (right); blots were probed with mAb 54.1 to gp91^{phox} and an antibody to p22^{phox}; β-actin serves as a loading control. **(d,e)** Flow cytometry of PMNs and monocytes **(d)** and EBV-B cells **(e)** from healthy controls **(d,e)**, patients with no gp91^{phox0} (gp91^{-/-}; **d,e**), patients with the *CYBB* mutations **(d)** and patients P1–P7 **(e)**, stained on the surface with mAb 7D5 to gp91^{phox} and isotype-matched control antibody (immunoglobulin G1 (IgG1)). Data are representative of two independent experiments **(a,d,e)**, two experiments **(b)** or three experiments **(c)**.

**Figure 6.**

Expression and function of mutant gp91^{phox} in cell lines. **(a)** Immunoblot analysis of CHO cells and CHO22 cells (CHO cells generated for the stable expression of untagged p22^{phox}) transduced with retroviral particles encoding wild-type gp91^{phox}, T178P gp91^{phox} or Q231P gp91^{phox}, then selected with puromycin; lysates were evaluated for gp91^{phox} (mAb 54.1), p22^{phox} (mAb NS5) and β-actin (loading control). **(b)** Flow cytometry of cell surface gp91^{phox} in untransduced CHO22 cells (top) and CHO22 cells expressing wild-type gp91^{phox}, Q231P gp91^{phox} or T178P gp91^{phox}, detected with mAb 7D5. **(c)** Immunoblot analysis of lysates (amount, above lanes) of wild-type PLB-985 cells (PLB WT) and PLB XR-CGD cells left untransduced (X) or transduced and selected as in **a** (X + gp91), then left undifferentiated (-) or differentiated into granulocytes by 6 d of induction with DMF (+); blots were probed for gp91^{phox} (mAb 54.1), p67^{phox} (to verify differentiation) and β-actin (loading control). **(d)** Immunoblot analysis of lysates (20 μg per well) of PLB-985 cells transduced as in **c** and differentiated into monocyte-like cells with vitamin D (Vit D) or into macrophage-like cells with a combination of vitamin D and PMA (below lanes); blots were probed for gp91^{phox} (mAb 54.1) and p67^{phox} (to verify differentiation). Far right, lysates of human PMNs (2.5 μg) serve as a control. Data are representative of three independent experiments.